

Discovery of two nearby post-T Tauri stellar associations

JIAMING LIU,¹ MIN FANG,² AND CHAO LIU^{3,4}

¹*Key Lab of Optical Astronomy, National Astronomical Observatories, CAS, Beijing 100101, China*

²*Department of Astronomy, University of Arizona, 933 North Cherry Avenue, Tucson, AZ 85721, USA*

³*Key Lab of Space Astronomy and Technology, National Astronomical Observatories, CAS, Beijing, 100101, China*

⁴*University of Chinese Academy of Sciences, Beijing 100049, China*

ABSTRACT

In this work we report the discovery of 2 new stellar associations in close vicinity of the Sun at roughly 180 and 150 pc. These two associations, named as u Tau assoc and e Tau assoc, were detected based on their clustering in a multi-dimensional parameter space including $\alpha, \delta, \mu_\alpha, \mu_\delta$ and ϖ of *Gaia*. The fitting of pre-main-sequence model isochrones in their color-magnitude diagrams suggests that the two associations are of about 50 Myr old and the group members lower than $\sim 0.8 M_\odot$ are at the stage of post-T Tauri.

Keywords: Young star clusters, Pre-main sequence, Pre-main sequence stars

1. INTRODUCTION

Stellar associations, as fundamental blocks of our Milky Way, will help us to understand the formation and evolution of the structures of the Milky Way. Nearby young associations are particularly important, and are excellent laboratories for studying the initial mass functions (IMF) in extremely low mass range (Gagné et al. 2018), formation and early evolution of planetary systems and brown dwarfs (BD) (Chauvin et al. 2015), since young objects of sub-stellar and planetary mass range are comparatively bright and easy to be detected. However, due to the low stellar density and large extension in the sky, nearby young associations and their members are hard to be identified. Members of them are newly formed in same molecular cloud and haven't been significantly perturbed by the Galaxy, thus they usually share some common properties such as age, chemical composition, distance and kinematics (Song et al. 2003; Torres et al. 2008; Gagné et al. 2018). Therefore, these stars will usually show significant concentration in multi-dimensional astrometric space and be identified as over-densities from its surrounding field stars (Fűrnkranz et al. 2019).

Recently, *Gaia* DR2 data, which provides position and G band (330-1050 nm) photometric data down to magnitude 21 for 1.7 billion stars, including parallax and proper motions for over 1.3 billion stars and radial velocity for stars brighter than 13 magnitude in G band (Gaia Collaboration et al. 2016, 2017, 2018), will definitely promote the membership completeness of current stellar associations and boost the discovery of new stellar associations. Here, we report the discovery of two new young associations near Taurus.

This work is arranged as follows. In §2, we describe the data and refine the membership of the associations. The population properties will be discussed in §3. Followed by a brief discussion in §4, and finally summary and conclusion in §5.

2. DATA AND MEMBERSHIP

2.1. Data Selection

During a study about the young stellar associations of Taurus (Liu J. et al. 2020, in preparing) with *Gaia* DR2 data, we notice that apart from those known associations, there are two likely stellar associations near Taurus, located at roughly 150 and 180 pc that haven't been realized before. The two candidates of associations that roughly centered to $(+21.21, -13.94)$ and $(+24.22, -24.02)$ of (μ_α, μ_δ) , are clearly notable from their surrounding field stars as outstanding over-densities in the proper motion space (see figure 1). Stars employed in this plot are selected by 50° to 65° of α , 0°

Corresponding author: Chao Liu
liuchao@nao.cas.cn; mfang@email.arizona.edu; jmlu@nao.cas.cn

¹ Jiaming Liu, LAMOST Fellow.

to 20° of δ , 15 to 35 mas/yr of μ_α , -30 to -5 mas/yr of μ_δ and 100 to 200 pc of distance. As the two associations are tightly clustered in the proper motion space, to refine their memberships, the data we selected are based on the following criteria: (1) all those sources around the center of these two associations with a radius of 5 mas/yr from the proper motion space, slightly larger than the radii of them; (2) a parallax quality of $\sigma_\varpi/\varpi \leq 0.1$; (3) the flux error of G_{RP} smaller than 5%; considering that the typical distance extension for nearby young associations are usually ~ 20 pc (Gagné et al. 2018), (4) the distance cut is set to be 100-200 pc from the Sun. In total we have 448 stars.

2.2. Membership

Membership refinement by their concentration in multiple astrometric space is the most commonly used method for associations showing clear over densities in the astrometric space. Considering members of the nearby associations are usually loosely concentrated in the spatial space, a “Friend-of-Friend” (“FOF”) algorithm of “ROCKSTAR”¹ is adopted (Behroozi et al. 2013). Based on the sample stars input, ROCKSTAR will automatically modify the linking-space between members of “friend” stars, divide them into several groups, and label those isolated individual stars out. Thus, with these 448 stars we selected above, we ruled out the surrounding field stars by eliminating isolated stars at each run time. After 3 iterations of the “ROCKSTAR”, The left stars are spatially concentrated in two groups (see figure 2), which contain 35 and 119 members, respectively. We regard them as u Tau assoc and e Tau assoc (see table 1 and 2 for detail information) hereafter. A reliability test of ROCKSTAR in refining memberships of the 2 associations is proven in the appendix. The ROCKSTAR can find out $\sim 95\%$ of the group members at a purity level of $\sim 90\%$, proved that the ROCKSTAR method is a effective way in refining memberships of Tau-assocs kind. Figure 2 shows the locations of the associations, the cyan asterisks indicate the stars of u Tau assoc and the purple crosses represent the members of e Tau assoc. The association u Tau as-

soc, located at roughly 180 pc from the Sun, is tightly concentrated in both α and δ (centered at 56.0° , 5.46°) and proper motion space. The e Tau assoc is located at 150 pc from the Sun, tightly concentrated in the proper motion space but largely extended in the α and δ space (centered at 57.69° , 10.16°).

2.3. Spectra Data

The spectra data adapted in this work is taken from LAMOST. The Large Sky Area Multi-Object Fibre Spectroscopic Telescope (LAMOST), is a 4m Schmidt telescope of the National Astronomical Observatories, located at Xinglong Observing Station, China. With 4000 fibers on board the focus, the LAMOST can observe nearly 4000 optical spectra in a 20 square degrees a time (Cui et al. 2012). Since 2012, the LAMOST has released its surveying data 7 times. The data that engaged in this work are taken from the recently released data DR5. LAMOST DR5 provides over 9 million spectra as well as a catalog of general stellar parameters derived from the spectra for over 5 million stars. With LAMOST data, we will discuss some properties of the associations later.

3. POPULATION PROPERTIES

3.1. Convergent Point

As a projection effect, the co-moving members of an association usually converge to a certain point of the celestial sphere, known as convergent point (CP; Galli et al. 2012). The CP point, ever since its first presented by Bohlin in 1916 (Smart 1968), has also been used as an important tool for testing membership of associations. Since then a lot of different methods have been introduced for its solution (Jones 1971; de Bruijne 1999; Galli et al. 2012). In order to confirm that these 2 new associations are not from the same group, we derive their convergent points of the equatorial coordinates. The CPs for u Tau assoc and e Tau assoc are $(98.06^\circ, -19.32^\circ) \pm (0.67^\circ, 0.36^\circ)$ and $(108.39^\circ, -33.23^\circ) \pm (0.54^\circ, 0.28^\circ)$, respectively. The difference of the convergent points is evident that the two associations, although close in the location and share similar properties, are indeed two separated ones.

3.2. Age and Mass

Figure 3 shows the CMDs for the 2 associations. The gray dots are the foreground stars in the same direction of them but within 100 pc from the Sun, and are regarded as main-sequence stars here. The foreground stars are selected based on the following criteria: 1. stars in the region of 0 - 20° of α and 50 - 65° of δ ; 2. $\sigma_\varpi/\varpi \leq 0.1$; 3. the flux error of G_{RP} smaller than

¹ ROCKSTAR is based on adaptive hierarchical refinement of friends-of-friends (FOF) groups in six phase-space dimensions, which allows for the tracking of high number density clusters, and divided all the stars into several groups excluding those stars that could not be vested in the star aggregates. It is designed to find out outlier structures that tightly connected in the 6 dimension space, as *Gaia* DR2 only provides radial velocity for bright stars with G band magnitude brighter than 13.0. Thus, to adopt ROCKSTAR, we set radial velocity as zero for all sample stars and keep the other 5D coordinates as $\alpha, \delta, \mu_\alpha, \mu_\delta$ and distances given by Bailer-Jones et al. (2018).

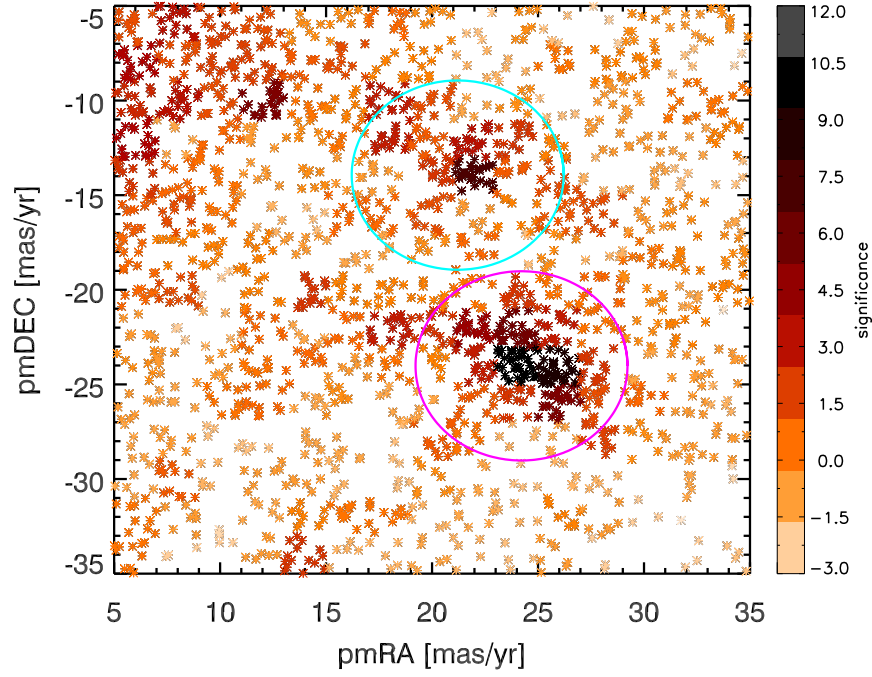


Figure 1. The location of the two associations in μ_α , μ_δ space. Based on their locations in the proper motion, stars are divided into a series bins of $2 \text{ mas/yr} \times 2 \text{ mas/yr}$, while colors of symbols in each bin denote the significance of them. Cyan and purple circles are 5 mas/yr region around the center of the potential associations.

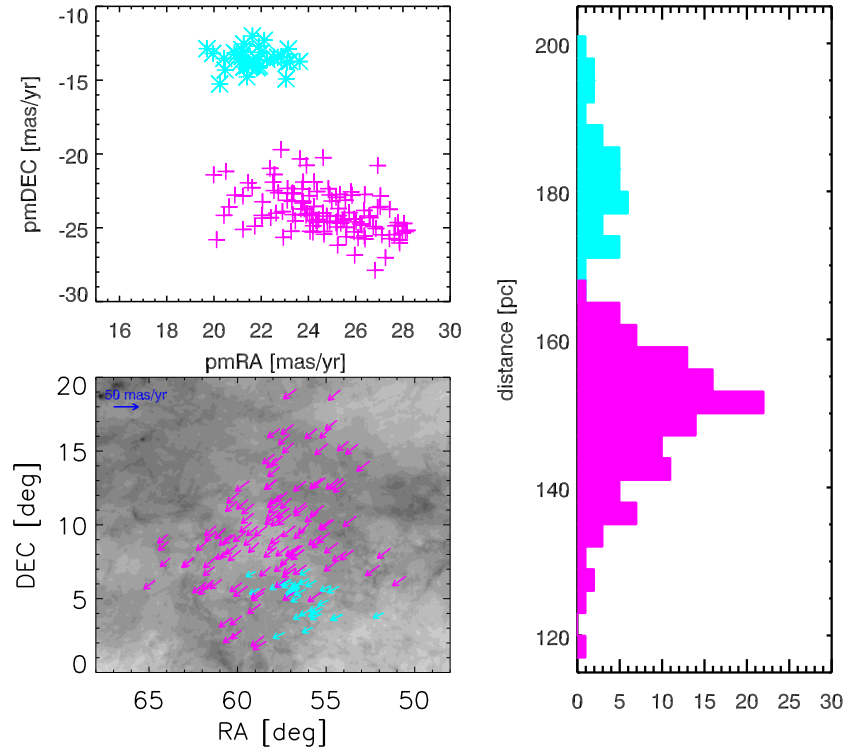


Figure 2. The location of the two associations at α , δ space (lower-left panel), μ_α , μ_δ space (upper-left panel) and distance distribution (right panel). Background contour in the lower-left panel are the $350 \mu\text{m}$ dust emission map of Planck.

5%; 4. stars in 100 pc from the Sun, in total we have 1934 stars. Asterisks and crosses represent for the members of the associations u Tau assoc and e Tau assoc, respectively. Interstellar extinction is corrected using the Galactic average extinction law of $R_V = 3.1$, where $R_V = A_V/E(B - V)$ is the total to selective coefficient. Since the V band interstellar extinction is about 0.7-1.0 mag/kpc in solar neighbourhood (Gottlieb and Upson 1969; Milne and Aller 1980; Wang et al. 2017), a mean value of 0.85 mag/kpc is taken here. Then for each individual star at distance D , its V -band extinction A_V should be $0.85 \times D$. Finally, with the extinction coefficient for *Gaia* G_{BP} and G_{RP} bands of $R_V = 3.1$ that provided by Wang and Chen (2019), the G_{BP} and G_{RP} extinction for each individual star of both foreground main-sequence stars and the associations members are corrected. The mean V band extinctions for u Tau assoc and e Tau assoc are 0.154 mag and 0.127 mag, respectively.

The blue dashed line in each panel are the best fitted isochrone of PARSEC (Bressan et al. 2012) of solar metallicity. The fit is done as follow: for each isochrone of certain age, select those stars within the color and absolute magnitude range of the isochrone. Distances of an isochrone to each of these stars are derived, as the number of stars inside the color and magnitude range is different from isochrone to isochrone, thus the isochrone with smallest mean distance to stars are regarded as the best-fit. The result showed that these two associations are both young, 50 Myr for u Tau assoc and 46 Myr for e Tau assoc. Actually, as a result of core fusion and convection, surface Lithium abundance will deplete with time, and can also be used to estimate age of PMS stars (Herbig 1965; Weymann & Sears 1965). But this method is not appropriate for LAMOST low-resolution spectra, whose resolution is ~ 1800 , hard to deduce the Lithium abundance accurately. Therefore Li-based method is not considered in this work.

In order to better confirm the result of the age estimation, we alternatively considered the semi-empirical pre-main-sequence model isochrones of Bell et al. (2014) for SDSS bands, which they derived base on the Pisa PMS isochrones of Tognelli et al. (2012). Realizing that over half of the stars lack of SDSS observations, thus we cross-match the members of Tau-assocs to PanSTARRS (Chambers et al. 2016), of which only 2 stars of e Tau assoc have no counterparts. But to control the security of the model fit, only those stars with good-quality measurements of PanSTARRS (quality flag of 4, 8 and 16) are conserved (32 stars of u Tau assoc and 106 stars of e Tau assoc). Then we transferred these photometric data of PanSTARRS to SDSS bands with method of

Tonry et al. (2012), of which the transition accuracy is better than 0.002 and 0.003 mag in r and i band, respectively. The model fit result is also shown in figure 3, and the age are estimated to be 58 and 54 Myr for u Tau assoc and e Tau assoc respectively, well agree with the age estimation of PARSEC.

Besides, the transition point (e.g. the Turn-On point: TON) from PMS to main-sequence (MS) can also be used to estimate age of young stellar groups. Because the TON point on the CMD will become flatter and drop to the main-sequence tracks as the stellar group growing old (Cignoni et al. 2010). Therefore, TON can also serve as an indicator of age for clusters that sufficiently young to contain PMS members. In light of this, the TON of PARSEC model is also considered as a validation of our age estimation. The result of this approach is shown in figure 4. TONs of the Tau-assocs are both consistent with that of the 50 Myr, with the TON point roughly correspond to a $\sim 0.8M_\odot$ star.

With the best fitted isochrones of PARSEC, stellar masses are then estimated. The mass range of the associations demonstrate that most of their members are low mass (sub-solar mass) with a few of them has masses larger than solar mass, and an upper limit of $\sim 6.0M_\odot$. Based on the masses of stars, we fit the present-day mass functions to a series of IMF (initial mass function) of Kroupa (2001), and the total mass of the 2 associations are estimated to be ~ 40 and $\sim 160 M_\odot$ respectively for u Tau assoc and e Tau assoc (see figure 5).

3.3. Radial Velocity and Metallicity

Radial velocity is an important parameter of kinematics, especially for stars of the associations. Since *Gaia* DR2 only provided the radial velocities for bright stars, 7 star in u Tau assoc and 29 in e Tau assoc have *Gaia* released radial velocities. We also searched members of the associations in the LAMOST DR5, and 23 stars of them are found in the LAMOST DR5 catalogue, but only 1 of them is new. In a word, we have 8 members of u Tau assoc and 29 members of e Tau assoc with radial velocity information. The histograms of the radial velocity for the associations are plotted in figure 6. A rough examination showed that the mean value of the radial velocity of u Tau assoc is 16 km/s with dispersion of 2 km/s, while for e Tau assoc the average value is 15 km/s and a dispersion of 5 km/s.

Besides radial velocity, LAMOST DR5 also provided metallicities for 7 stars in u Tau assoc and 16 in e Tau assoc. The mean metallicity for u Tau assoc and e Tau assoc are 0.03 and 0.03 dex, respectively.

4. DISCUSSION

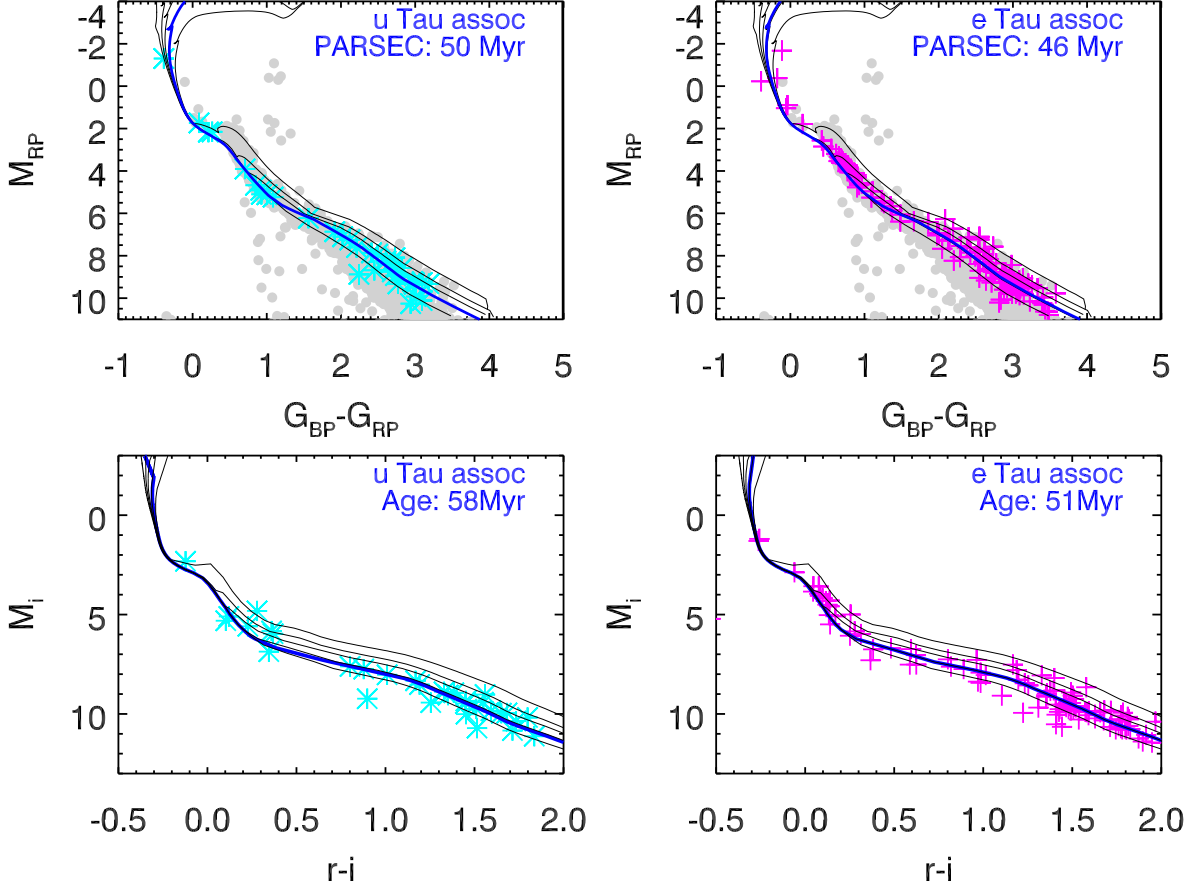


Figure 3. The color-magnitude diagram of Tau-associations. Gray dots are the foreground main-sequence stars in the same direction. Cyan asterisks denote the u Tau assoc, while purple crosses indicate members of e Tau assoc. The blue solid line are the best fitted isochrones of PARSEC (upper panels) and model of Bell et al. (2014) (lower panels). The thin black lines from the top to the bottom in each panel denote isochrones of 10, 20, 30, 50 and 100 Myr.

Associations, especially those nearby associations are the ideal laboratory for studying stellar kinematics and evolution of stars in groups, therefore, efforts have been taken for searching more new associations, especially after the data release of *Gaia*. Quite soon after the first data release of *Gaia*, Oh et al. (2017) have applied a marginalized likelihood ratio test to the Tycho-*Gaia* Astrometric Solution (TGAS), searching for co-moving pairs from field stars. From 10,606 unique stars, by a connection radius of 10 pc, they find 13,085 co-moving star pairs. Later, Faherty et al. (2018) pushed the work forward and reexamined the result of Oh et al. (2017) with the bayesian method BANYAN Σ , apart from those associations of already known, they also reported over 20 potential new stellar groups. Among their potential stars in groups, 10 members of the association e Tau assoc of this work are included, but were separated in 3 different groups. A likely reason for this is that for the very time of their work, TGAS is short in stars, as e Tau assoc is largely extended in the space, it's natural that

the members were not linked together and divided into several parts. On the other hand, their work also confirmed the fact that these stars are clustered in groups.

A 2 arcsec radius cross-match with SIMBAD show that these 2 associations in total contains 43 counterparts, including 3 B3, 4 B9, 1 A1, 3 A5, 8 F type, 7 G type, 3 K type, 1 M type stars (13 with no spectra type information). This is consistent with the mass estimation results in section 3.2 that the associations of this work contains a few stars of several solar masses. Tetzlaff et al. (2011) published a catalogue of young *Hipparcos* stars within 3 kpc from the Sun. 4 of the 43 SIMBAD sources in this work are included, and the age are estimated as 5.7, 7.0, 13.4 and 37.8 Myr, which are younger than the ages of this work. The difference is understandable since both works using different distances. In Tetzlaff et al. (2011), they adopted the distances from *Hipparcos*, with seven sets of evolutionary models, they derived the median ages from them (see details in Tetzlaff et al. (2011)). For two sources with

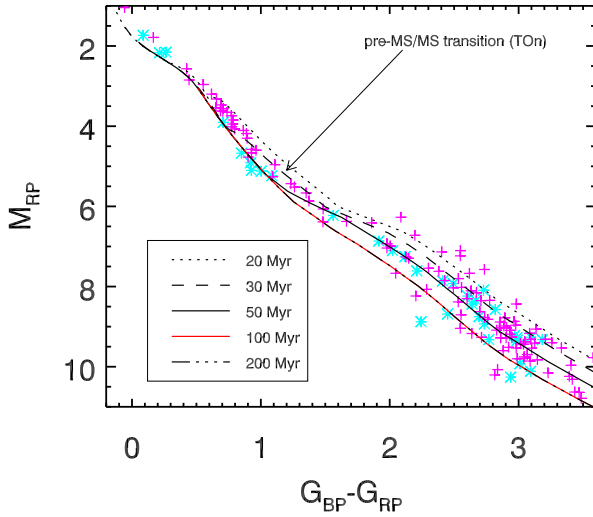


Figure 4. Pre-main sequence tracks of different ages given by PARSEC, also plotted are the members of Tau-assocs with symbols defined the same as before.

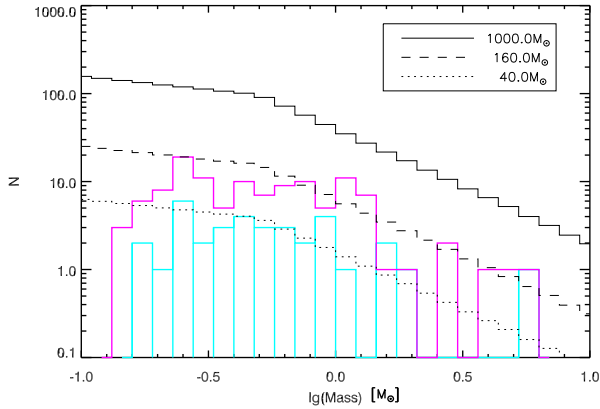


Figure 5. Mass estimation of the associations based on the IMF model of Kroupa (2001).

ages of 5.7 or 7.0 Myr in Tetzlaff et al. (2011), there are large difference between the distances from *Hipparcos* and *Gaia* with the distances from *Hipparcos* being 26% and 16%, respectively, larger than those from *Gaia*. This can result in higher luminosity and younger ages in Tetzlaff et al. (2011) than this work. Furthermore, the age of each association in this work is estimated as a whole from CMD or the TON, which should provide a better age estimation than just using individual stars.

Early in 1978, Herbig introduced post T Tauri stars (PTTS) in order to explain the lack of “older” pre-main sequence T Tauri stars with age older than 5 – 10 Myr

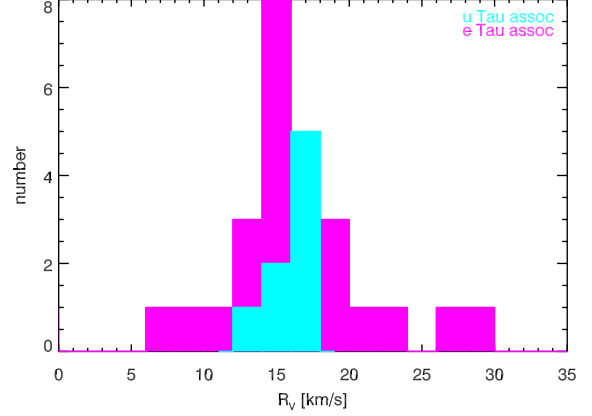


Figure 6. Radial velocities histogram of Tau-assocs. Cyan for u Tau assoc, and purple for e Tau assoc.

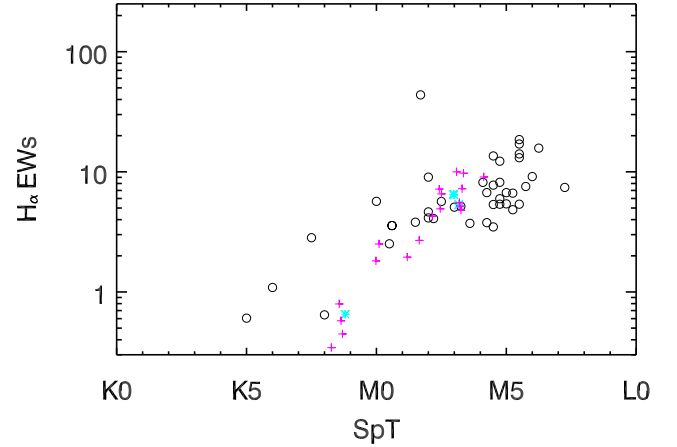


Figure 7. The H α Equivalent width of Tau-assocs members (cyan asterisks for u Tau assoc and purple crosses for e Tau assoc) compared with those of known Taurus PMS stars of no disk (Esplin et al. 2014, shown as open black circles).

in star forming regions (Herbig 1978). As the distinct characteristics of T Tauri stars, e.g. strong H α emission, high surface lithium abundance, irregular variability, and color excess of infrared as well as X-ray emission (Walter 1986) are absented at stage of zero-age main sequence (ZAMS), he argued that the PTTS should show intermediate or moderate value of these characteristics. Jensen (2001) thought that PTTS are stars older than T Tauri but haven’t reach zero-age main sequence (ZAMS), and discussed the properties of them in his work. He stated that to certificate the validity of PTTS, apart from age estimation, the validity of PTTS should be further confirmed by at least one or two characteristics of T Tauri stars.

As the age of the Tau-assocs are estimated to be 50 Myr, stars under the TOn ($\sim 0.8M_{\odot}$) should be post-T Tauri stars. To certificate the validity, spectra of the Tau-assocs observed by LAMOST is examined. In total 44 of them has been observed, their equivalent with of H α line confirmed the transition from absorption to emission is roughly around the TOn. And the 18 stars with mass lower than the TOn mass do show obviously H α emission feature. Compared their H α equivalent width to that of previous known T Tauri stars with no circumstellar disk (Esplin et al. 2014), it shows that the intensities are comparatively moderate to that of T Tauri stars (see figure 7), manifesting their youth properties.

5. SUMMARY AND CONCLUSIONS

In this work, with *Gaia* DR2 astrometric data, by searching over densities of nearby stars in the multi-phase space, we find 2 new young stellar associations, u Tau assoc and e Tau assoc, that haven't been noticed before. The two associations are quite close to each other, but could be clearly separated. Members of u Tau assoc are tightly concentrated in both α, δ and $\mu_{\alpha}, \mu_{\delta}$ space, while the members of e Tau assoc, although also concentrated in the proper motions space, is more extended in the α and δ space within nearly 200 square degrees. These two associations are of solar metallicity

and young, with their best fitted isochrone ages are of about 50 Myr. From the fitting PMS model isochrones, the transition from Pre-main sequence to main sequence can be identified at $\sim 0.8 M_{\odot}$, and members lower than $\sim 0.8 M_{\odot}$ are at the stage of post T Tauri.

6. ACKNOWLEDGEMENT

We thank the anonymous referee for very helpful suggestions and comments. Quite a substantial data processing of this work are executed through the software of TOPCAT (Taylor 2005). This work is supported by the National Natural Science Foundation of China (NSFC) with grant No. 11835057. Guoshoujing Telescope (the Large Sky Area Multi-Object Fiber Spectroscopic Telescope LAMOST) is a National Major Scientific Project built by the Chinese Academy of Sciences. Funding for the project has been provided by the National Development and Reform Commission. LAMOST is operated and managed by the National Astronomical Observatories, Chinese Academy of Sciences. This work has made use of data from the European Space Agency (ESA) mission *Gaia* (<https://www.cosmos.esa.int/gaia>), processed by the *Gaia* Data Processing and Analysis Consortium (DPAC, <https://www.cosmos.esa.int/web/gaia/dpac/consortium>). Funding for the DPAC has been provided by national institutions, in particular the institutions participating in the *Gaia* Multilateral Agreement.

APPENDIX

A. RELIABILITY TEST OF ROCKSTAR

The purpose of ROCKSTAR we employed in this work is to refine the memberships and eliminated contaminations of the associations rather than discover associations, since we knew the two associations are clearly visible in the proper motion space. In considering that the ROCKSTAR code is not originally designed to handle associations, therefore, a test about the effectiveness of ROCKSTAR is necessary. Given that young associations will be questioned about the completeness and contamination, a man-made artificial testing association will be much better. Thus, we randomly created a testing group of 50 stars of the same general properties of Tau-assocs (u Tau assoc and e Tau assoc) and a larger region of field stars surround them, also with likely properties as those field stars around Tau-assocs. With same selecting criteria as searching for them and also run ROCKSTAR for 3 times. We repeat this procedure 10 times, and showed the result in the figure 8.

The result show that in 10 times of testing, ROCKSTAR can find out $\sim 95\%$ of the group members at a purity level of $\sim 90\%$, proved that the code is an effective way in refining memberships of Tau-assocs kind. By this We mean that the ROCKSTAR code is an effective way in searching for members of Tau-assocs-like, but not for all the associations.

REFERENCES

- | | |
|-----------------------------------------------------------------------------------------------------|---------------------------------------------------------------------------|
| Bailer-Jones, C. A. L., Rybizki, J., Fouesneau, M.,
Mantelet, G., & Andrae, R. 2018, AJ, 156, 58 | Bell, C. P. M., Rees, J. M., Naylor, T., et al. 2014,
MNRAS, 445, 3496 |
| Behroozi, P. S., Wechsler, R. H., & Wu, H.-Y. 2013, ApJ,
762, 109 | Bressan, A., Marigo, P., Girardi, L., et al. 2012, MNRAS,
427, 127 |

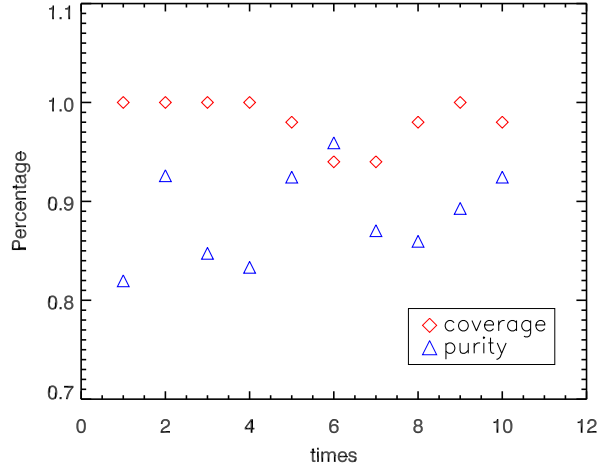


Figure 8. The result of searching for the created association. Coverage means how many of the 50 group stars are located in the result. Purity is the group members left to that of total number of stars left in the process.

- Briceño, C., Hartmann, L., Stauffer, J., & Martín, E. 1998, *AJ*, 115, 2074
- Briceño, C., Calvet, N., Kenyon, S., & Hartmann, L. 1999, *AJ*, 118, 1354
- Briceño, C., Luhman, K. L., Hartmann, L., Stauffer, J. R., & Kirkpatrick, J. D. 2002, *ApJ*, 580, 317
- Cardelli, J. A., Clayton, G. C., & Mathis, J. S. 1989, *ApJ*, 345, 245
- Chauvin, G., Vigan, A., Bonnefoy, M., et al. 2015, *A&A*, 573, A127.
- Chambers, K. C., Magnier, E. A., Metcalfe, N., et al. 2016, *arXiv:1612.05560*
- Cignoni, M., Tosi, M., Sabbi, E., et al. 2010, *ApJL*, 712, L63
- Cui, X.-Q., et al. 2012, *Research in Astronomy and Astrophysics*, 12, 1197
- de Bruijne, J. H. J. 1999, *MNRAS*, 306, 381
- Dotter, A., Chaboyer, B., Jevremović, D., et al. 2008, *ApJS*, 178, 89
- Esplin, T. L., Luhman, K. L., & Mamajek, E. E. 2014, *ApJ*, 784, 126
- Esplin, T. L., & Luhman, K. L. 2017, *AJ*, 154, 134
- Esplin, T. L., Luhman, K. L., Faherty, J. K., Mamajek, E. E., & Bochanski, J. J. 2017, *AJ*, 154, 46
- Faherty, J. K., Bochanski, J. J., Gagné, J., et al. 2018, *ApJ*, 863, 91
- Fang, M., Kim, J. S., Pascucci, I., et al. 2017, *AJ*, 153, 188
- Feiden, G. A., Jones, J., & Chaboyer, B. 2015, 18th Cambridge Workshop on Cool Stars, Stellar Systems, and the Sun, 18, 171
- Fürnkranz, V., Meingast, S., & Alves, J. 2019, *A&A*, 624, L11
- Gagné, J., Mamajek, E. E., Malo, L., et al. 2018, *ApJ*, 856, 23
- Galli, P. A. B., Teixeira, R., Ducourant, C., Bertout, C., & Benevides-Soares, P. 2012, *A&A*, 538, A23
- Galli, P. A. B., Loinard, L., Ortiz-Léon, G. N., et al. 2018, *ApJ*, 859, 33
- Gaia Collaboration et al., 2016, *A&A*, 595, A2
- Gaia Collaboration et al., 2017, *A&A*, 601, A19
- Gaia Collaboration, Brown, A. G. A., Vallenari, A., et al. 2018, *A&A*, 616, A1
- Gottlieb, D. M., & Upson, W. L. 1969, *ApJ*, 157, 611
- Guieu, S., Dougados, C., Monin, J.-L., Magnier, E., & Martín, E. L. 2006, *A&A*, 446, 485
- Herbig, G. H. 1965, *ApJ*, 141, 588
- Herbig, G. H. 1978, *Problems of Physics and Evolution of the Universe*, 171
- Jensen, E. L. N. 2001, *Young Stars Near Earth: Progress and Prospects*, 244, 3
- Joncour, I., Duchêne, G., & Moraux, E. 2017, *A&A*, 599, A14
- Jones, D. H. P. 1971, *MNRAS*, 152, 231
- Kraus, A. L., Herczeg, G. J., Rizzuto, A. C., et al. 2017, *ApJ*, 838, 150
- Kroupa, P. 2001, *MNRAS*, 322, 231
- Lim, B., Sung, H., Kim, J. S., et al. 2016, *ApJ*, 831, 116
- Luhman, K. L. 2004, *ApJ*, 617, 1216.
- Luhman, K. L. 2007, *ApJS*, 173, 104.
- Luhman, K. L., Mamajek, E. E., Allen, P. R., & Cruz, K. L. 2009, *ApJ*, 703, 399
- Luhman, K. L., Mamajek, E. E., Shukla, S. J., & Loutrel, N. P. 2017, *AJ*, 153, 46
- Luhman, K. L. 2018, *AJ*, 156, 271

- Luo, A.-L., Zhang, H.-T., Zhao, Y.-H., et al. 2012, *Research in Astronomy and Astrophysics*, 12, 1243
- Milne, D. K., & Aller, L. H. 1980, *AJ*, 85, 17
- Murphy, S. J., & Lawson, W. A. 2015, *MNRAS*, 447, 1267
- Oh, S., Price-Whelan, A. M., Hogg, D. W., Morton, T. D., & Spergel, D. N. 2017, *AJ*, 153, 257
- Ortega, V. G., Jilinski, E., de la Reza, R., & Bazzanella, B. 2009, *AJ*, 137, 3922
- Röser, S., Schilbach, E., Goldman, B., et al. 2018, *A&A*, 614, A81
- Smart, W. M. 1968, London: Longmans, 1968,
- Song, I., Zuckerman, B., & Bessell, M. S. 2003, *ApJ*, 599, 342
- Stauffer, J. R. 1980, *AJ*, 85, 1341
- Su, D.-Q., & Cui, X.-Q. 2004, *ChJA&A*, 4, 1
- Taylor, M. B. 2005, *Astronomical Data Analysis Software and Systems XIV*, 29
- Tetzlaff, N., Neuhauser, R., & Hohle, M. M. 2011, *MNRAS*, 410, 190
- Tognelli, E., Degl’Innocenti, S., & Prada Moroni, P. G. 2012, *A&A*, 548, A41
- Tonry, J. L., Stubbs, C. W., Lykke, K. R., et al. 2012, *ApJ*, 750, 99
- Torres, G., Winn, J. N., & Holman, M. J. 2008, *ApJ*, 677, 1324
- Walter, F. M. 1986, *ApJ*, 306, 573
- Wang, S., Jiang, B. W., Zhao, H., et al. 2017, *ApJ*, 848, 106
- Wang, S., & Chen, X. 2019, *ApJ*, 877, 116
- Weymann, R., & Sears, R. L. 1965, *ApJ*, 142, 174
- Wichmann, R., Bastian, U., Krautter, J., Jankovics, I., & Rucinski, S. M. 1998, *MNRAS*, 301, L39

Table 2. Members of e Tau assoc

GAIA ID	other names	RAJ2000 (deg)	DEJ2000 (deg)	pmRA (mas/yr)	pmDEC (mas/yr)	Distance (pc)	R_V (km/s)	Sp-Type
9509336766831744		50.505	6.508	26.382	-22.743	133.808		
10942515813999488	HD 21194	51.362	8.427	26.855	-25.050	136.770	19.460	F5
9993671639120256	BD+06 533	51.991	7.255	27.982	-25.361	134.707		F8
41872327659525504		52.540	14.325	26.191	-24.738	148.766		
42352367565698304		53.199	15.473	24.905	-24.567	150.619		
13078626388631424	V* V1267 Tau	53.298	10.599	26.370	-25.552	136.872	15.080	K3
11397988505713536	HD 22073	53.444	8.291	27.040	-23.569	146.711		A5
42440500294245120		53.754	15.662	22.055	-23.234	156.706		
11472617857575552		53.869	8.199	27.438	-23.753	142.724		
40695158727074048		53.895	12.884	24.773	-24.208	163.725		
40705848902910464		54.027	13.128	27.849	-25.848	144.380		
57153099745350912		54.208	19.135	24.200	-24.869	150.991		
40726224227818240		54.306	13.125	25.209	-24.951	156.096		
11522435182853120		54.325	8.793	27.684	-24.865	142.689		
3277897741565006976		54.382	7.551	25.466	-24.476	145.419		
44258027374647808		54.396	17.088	23.681	-23.716	158.050	12.740	K7
12343637226131584	TYC 660-709-1	54.576	10.338	26.748	-24.923	146.051	14.560	G9
12355628774864128		54.704	10.363	25.724	-23.969	147.480		
44034311118104320		54.718	16.595	22.937	-25.649	158.159		
11959323551830912		54.793	9.466	24.434	-24.441	144.029	17.040	K3
41651772500169984	TYC 1235-156-1	54.915	15.499	25.957	-26.861	155.433	15.870	
38088873789758720	BD+12 500	55.042	13.199	25.527	-24.403	150.120	14.170	F8
11888473771374848		55.143	9.114	23.332	-24.108	147.665		
37195348793250048		55.154	11.293	27.113	-25.476	142.693		
38076641722829440	TYC 663-362-1	55.241	13.151	24.656	-25.443	147.577	13.360	
3275164390018316288		55.273	5.454	26.928	-23.628	141.578		
11985196435903488		55.283	9.285	24.988	-23.192	149.482		
36420502331404160	TYC 660-135-1	55.442	10.908	26.399	-25.756	140.121	14.500	
44057778819482496		55.515	16.528	24.365	-24.625	150.486		
36103396308075776		55.966	10.088	22.041	-24.349	150.297		
36530487856056704		56.072	11.303	26.253	-24.827	136.375		
3277686910210391296	2MASS J03442859+0716	56.119	7.270	25.801	-22.564	150.709		M4
36537737760831744		56.126	11.501	25.259	-24.176	149.959		
37844713488859264		56.147	12.959	24.614	-24.007	154.850		
36034023996411392		56.179	9.738	22.636	-24.009	150.274		
3278197770802258944	HD 23376	56.246	8.320	26.612	-24.306	144.644	16.490	G5
3278197766505583232	TYC 658-1007-2	56.246	8.321	26.577	-24.198	142.418	20.640	
3278487148518773248		56.306	8.616	26.363	-23.826	155.014		

Table 2 continued

Table 2 (continued)

GAIA ID	other names	RAJ2000 (deg)	DEJ2000 (deg)	pmRA (mas/yr)	pmDEC (mas/yr)	Distance (pc)	R _V (km/s)	Sp-Type
3278300987456845440	TYC 658-828-1	56.467	8.541	27.783	-24.644	131.926	15.590	
3278489313182286720		56.501	8.609	27.791	-24.834	135.925		
50970717660507008		56.690	19.189	25.563	-23.138	154.909		
3277287615693093376		56.717	7.078	27.049	-22.842	150.719		
3277313144978675840		56.726	7.344	25.167	-22.944	142.686		
3302676747927557504		56.741	9.945	27.262	-27.025	137.566		
3276420135378285056		56.798	5.440	22.837	-19.710	163.312		
42956995881088256		56.847	15.557	21.727	-24.897	157.735		
43660752042391680		56.849	16.808	24.806	-24.601	154.295		
3278204402232390528	BD+07 543	56.880	7.957	25.369	-24.690	155.451	14.640	F8
36203417507399808		56.966	10.724	27.642	-25.464	158.885		
36901298152686080	TYC 661-560-1	56.974	11.816	21.230	-25.115	154.141	15.450	
43059486684334208		57.043	16.145	23.268	-25.243	159.908		
36290072767519232	* e Tau	57.068	11.143	25.269	-23.695	128.770		B3V
36290107127257344	TYC 661-1404-1	57.070	11.145	25.616	-24.972	137.914	19.560	F3Vn
3278259858850059264	TYC 658-922-1	57.131	8.527	25.327	-22.738	151.878	8.520	G7
36941189808895872		57.184	12.220	23.753	-23.215	159.044	11.880	K7
3276628183593979904		57.218	6.342	23.643	-20.334	155.848		
3277330153049126400		57.228	7.465	24.847	-22.347	150.250		
3302817966452511616		57.425	10.591	24.606	-24.003	149.917		
3302396166303947904	HD 23990	57.444	9.407	25.165	-24.660	147.495		B9
39846683645349376		57.460	14.682	22.024	-24.158	154.757		
36924353537157632		57.522	12.071	24.224	-23.552	153.293		
36701702432783616		57.572	11.496	24.337	-24.516	150.262		
43458167025621504	2MASS J03502840+1631	57.618	16.521	24.242	-21.892	146.359	7.390	G5IV
39513359823463680		57.620	13.937	23.942	-24.043	149.477		
3302299134402909056		57.638	8.930	24.037	-22.827	154.236		
36724620378249984		57.683	11.809	22.542	-22.481	165.514		
36595943156045824	BD+10 496	57.711	11.002	24.137	-24.167	151.392	14.960	F8
3302822811175649664		57.724	10.702	26.015	-24.606	141.009		
39641487287397632		57.772	14.526	20.639	-23.587	154.918		
3301516179044339840		57.786	8.489	25.935	-24.427	137.591		
37136524921755904		57.793	13.046	23.101	-23.138	162.124		
37136834159399808	V* V766 Tau	57.816	13.046	23.769	-23.228	160.771		B9pSi
39841357885932288	TYC 664-136-1	57.915	14.797	23.833	-23.721	159.686	28.720	
3277156567650183680		58.149	7.156	21.228	-22.856	158.009		
3270343546928113664	HD 24456	58.376	2.119	26.933	-20.785	138.680		B9V
3273850404904742912	TYC 72-816-1	58.449	5.707	28.184	-25.182	132.266	27.560	
3270377941026192768		58.506	2.484	26.104	-25.683	124.607		
3273648919399332608	TYC 72-620-1	58.513	5.431	24.625	-20.253	142.703	22.210	

Table 2 continued

Table 2 (continued)

GAIA ID	other names	RAJ2000 (deg)	DEJ2000 (deg)	pmRA (mas/yr)	pmDEC (mas/yr)	Distance (pc)	R _V (km/s)	Sp-Type
3273169120012500736		58.707	4.624	25.847	-22.798	141.751		
3301633517550972032		58.811	8.800	20.422	-24.161	154.244		
3302850402044815104		58.836	9.921	23.750	-23.323	151.633		
3301687599779043584		58.933	9.301	25.201	-24.605	149.626		
3303308245556503296	HD 286374	59.080	11.420	24.048	-24.124	152.306	13.600	F5
3303061851874905088	HD 286380	59.086	10.797	24.658	-25.252	147.681	14.650	G5
3302885135443350144		59.206	10.174	23.899	-24.142	150.217		
38398936068862464	TYC 665-150-1	59.339	12.971	28.046	-24.709	152.421		G0
3303319927869595264		59.412	11.709	23.298	-23.208	154.757		
3273771824183136256		59.428	5.856	28.109	-25.250	126.075		
3302063667115147008	2MASS J03581272+0932	59.553	9.540	24.321	-24.493	146.782	16.120	K3
3273802232551662336		59.748	6.092	24.363	-22.545	150.096		
3272119941104628352		59.750	3.837	23.782	-21.905	156.004		
3259900660364779392		59.767	2.881	21.447	-21.952	142.016		
3301312838112630400		59.814	8.289	25.603	-25.603	149.855		
3304906145189468416	TYC 662-217-1	59.926	12.169	24.066	-25.242	148.495	15.290	
3304619413175027968		60.004	11.611	24.188	-25.297	146.915		
3301396126118384768		60.013	8.653	23.291	-22.675	158.536		
3259830325980399744		60.132	2.593	23.916	-20.774	152.736		
3302018999455336192		60.158	9.367	22.724	-22.632	157.019		
3301329949262394624		60.292	8.406	23.114	-22.334	152.465		
3301831773241303552	BD+08 616	60.339	9.334	25.238	-26.184	155.343	42.580	F8
3272433615452990848		60.347	3.709	24.897	-22.773	140.743		
3298319348986238464		60.553	8.294	23.378	-22.681	150.586		
3301945366536236416		60.698	9.776	20.112	-25.812	146.839		
3297800516936921344		60.738	6.383	27.282	-26.218	135.379	-35.940	
3297045667844723712		60.893	6.298	23.739	-22.357	142.644		
3298606905637432576		61.165	7.866	26.820	-27.881	158.535		
3301900595797205632		61.206	9.585	22.404	-24.313	150.938		
3301974331795653888		61.211	9.936	22.900	-23.903	150.802		
3297959396367266560		61.304	7.172	22.500	-21.909	157.938		
3297032886022084864		61.344	6.259	23.325	-22.646	153.044		
3296973134437145984		61.436	6.014	27.429	-25.740	161.976		
3298826700586330240		61.667	8.941	23.444	-24.541	138.867		
3297062675915933696		61.753	6.119	27.861	-26.029	119.267		
3298371507070141056	TYC 666-80-1	62.448	7.801	21.622	-22.284	157.801	19.060	
3297619097518627968	HD 26323	62.529	7.698	22.376	-20.975	161.069		B9
3297666204719373440		63.798	7.764	20.502	-21.183	163.552		
3299306676067811200	* mu. Tau	63.884	8.892	20.881	-22.789	149.992		B3IV
3300180959610801536		63.944	9.357	19.986	-21.413	163.528		
3285243784909511168		64.650	6.244	22.561	-21.392	159.112		